Weaver, P.P.E., Schmincke, H.-U., Firth, J.V., and Duffield, W. (Eds.), 1998
Proceedings of the Ocean Drilling Program, Scientific Results, Vol. 157

30. SEDIMENTATION ON THE MADEIRA ABYSSAL PLAIN: EOCENE–PLEISTOCENE HISTORY OF TURBIDITE INFILL[1]

S.M. Lebreiro,[2] P.P.E. Weaver,[2] and R.W. Howe[2]

ABSTRACT

The sedimentary infill of the Madeira Abyssal Plain is analyzed in detail from the upper Eocene to Holocene at Sites 950, 951, and 952. In addition to the three turbidite groups (organic, volcanic, and calcareous) described in previous publications, gray nonvolcanic, brown and volcaniclastic turbidite groups were also recognized. Site 950 shows the longest sequence beginning with emplacement of two coarse volcaniclastic turbidites in the late Eocene. This was followed by a long interval of pelagic clay deposition until at least the end of the Oligocene. During this time volcanic ash was added from the now-extinct Cruiser/Hyeres/Great Meteor volcanic seamounts to the west. A hiatus in the lower Miocene rock is associated with the deposition of three coarse calcarenites at Site 950, also believed to be from the seamounts.

The uppermost calcarenite is a clear marker bed at 16 Ma. Sites 951 and 952 comprise thick sequences of relatively thin organic turbidites through the lower Miocene sequence, representing early infill of the fracture zone valleys in which they were drilled. Many sequences of flows can be correlated between all three sites from the middle Miocene to Holocene, although a series of brown turbidites occurring during the late Miocene (6.5–13 Ma) at Site 950 is less easy to trace. Volcanic turbidites are rare or very thin prior to 7 Ma, but common and thick after this time. Gray nonvolcanic turbidites are found in four limited intervals between 10.5–14.6 Ma, 5.6–7.4 Ma, 3.8–4.2 Ma, and 1.4–1.2 Ma, and include the thickest turbidites of all (11 m at Site 952).

The pelagic interbeds reveal the history of the carbonate compensation depth (CCD) which was shallower than the abyssal plain depth until ~8 Ma. Then the CCD deepened slightly, deepening again at ~5 Ma and finally entered the Pliocene/Pleistocene oscillatory mode at ~3.5 Ma. After this time alternating clays and marls or oozes were deposited.

INTRODUCTION

The Madeira Abyssal Plain (MAP) was one of a number of sites chosen in the late 1970s to study the feasibility of disposal of high-level radioactive wastes in the ocean. Although this study has now been concluded, it left a legacy of data and sedimentary models that has given great insight into deep-sea basin development (see review by Weaver et al., 1989). The main results to emerge from this work are as follows:

1. Through the last 0.75 m.y. the turbidite infill of the plain is composed of thick units deposited from individual turbidity flows, which enter the area at frequencies determined by climate and sea-level change (Weaver and Kuijpers, 1983). Each sea-level change, both up and down, is associated with a single turbidite unit, except in a very few cases where two turbidites may lie adjacent to each other (Weaver et al., 1992).

2. The turbidites fall into three distinct groups: volcanic-rich (gray with high Ti, Fe, Mg, and Zr) turbidites, organic-rich (olive green with high Si, Al, K, and Li) turbidites, and calcium-carbonate-rich (white with high Ca and Sr; Jarvis and Higgs, 1987) turbidites. These groups represent different sediment sources: the volcanic-rich ones from the oceanic islands of the Canaries and Madeira (Weaver and Rothwell, 1987), the organic-rich ones probably from the upwelling cells off northwest Africa (Weaver and Rothwell, 1987) and the calcium-carbonate–rich ones from the Cruiser/Hyeres/Great Meteor chain of seamounts to the west of the plain (Weaver et al., 1992).

3. The turbidites have silty or sandy bases proximally to their sources, but the upper layers of the turbidites are essentially ungraded muds, which may suggest deposition from high-density nonturbulent flows (McCave and Jones, 1988).

4. Turbidity current pathways can be determined from grain-size analyses of the turbidite bases, the coarsest samples indicating the most proximal parts of the flow. These show entry points from the northeast, east, and west (Weaver and Rothwell, 1987). Thickness of flows is not a good indicator of source direction as the turbidite muds pond, and preferentially infill any deeps in the basin floor.

5. The turbidites show the effects of early diagenesis, with relict oxidation fronts, associated metal concentrations and redox-related mobilization of trace elements, (Wilson et al., 1985; Thomson et al., 1987; Jarvis and Higgs, 1987). These effects are much more apparent in the organic-rich turbidites, which may develop striking color differences between the sediment above and below the oxidation front.

6. Through the Quaternary sediments, the turbidites are separated by pelagic units that alternate between pelagic marls (or oozes) and pelagic clays. These represent changing bottom-water masses associated with climate change (Weaver and Kuijpers, 1983).

Geological Setting

The MAP forms the deepest part of the Canary Basin with a water depth of 5400 m. The plain covers an area of 400 km (north-south) by 200 km (east-west) across which elevation changes by <10 m. To the

[1]Weaver, P.P.E., Schmincke, H.-U., Firth, J.V., and Duffield, W. (Eds.) 1998. *Proc. ODP, Sci. Results*, 157: College Station, TX (Ocean Drilling Program).

[2]Southampton Oceanographic Centre, Empress Dock, Southampton SO14 3ZH, United Kingdom. (Present address: CSIC-Instituto de Ciencias del Mar, Dept. de Geologia y Marina Oceanografia Fisica, Paseo Juan de Borbon, s/n 08039 Barcelona, Spain. lebreiro@icm.csic.es).

west of the plain the topography rises toward a north-south–trending chain of seamounts—the Great Meteor to Atlantis Chain (Verhoef and Collette, 1983)—and beyond these it begins to rise toward the Mid-Atlantic Ridge. To the north it rises toward the Madeira-Tore Rise. The Cape Verde Rise lies to the south; the northwest African continental rise, to the east (Searle, 1987). A few large sediment draped hills protrude through the plain cover to form isolated hills on the plain. The age of the crust beneath the MAP is mid- to Late Cretaceous (~116–77 Ma; Searle, 1987), and two ancient crustal fracture zone valleys—Cruiser and Charis—can still be traced running west-northwest–east-southeast (Fig. 1). Numerous seismic profiles across the plain (Searle, 1987; Rothwell et al., Chap. 28, this volume) show the crust to be draped by ~200 m of presumed pelagic clay. It is this draped topography that has been infilled by the turbidite sequence. The seismic data show the turbidite sequence to average 350 m in thickness, although in some basement deeps it may reach as much as 530 m. The turbidite sequence varies from being strongly acoustically laminated near the top to poorly stratified or even transparent near the base (Duin and Kuijpers, 1983). This suggests some changes in composition with depth.

Drilling Objectives

The drilling of the MAP was aimed at testing the above sedimentary models through the whole time interval of turbidite deposition in order to determine the erosional history of a large submarine basin. We also wished to date the sharp change from pelagic drape sediments to turbidite infill, which presumably represents a major change in sedimentation within the basin. A combination of the seismic interpretations (Rothwell et al., Chap. 28, this volume) with the sedimentological information presented here, and the stratigraphic information from Howe and Splendorio-Levy (Chap. 29, this volume) will provide the information needed to determine sediment budgets for material eroded from the various mass wasting sources.

CORE LOCATION

Three sites were drilled during Leg 157 on the abyssal plain, all within fracture zone valleys where connections to the northwest African Margin should have been continuous through time (Rothwell et al., Chap. 28, this volume). Site 950 (31°9.01′N, 25°36.00′W, 5437.8 m) is located on the southern edge of the Cruiser Fracture Zone Valley (Fig. 1). Site 951 (32°1.89′N, 24°52.23′W, 5449.4 m) is located in the central basin to the north, within the Charis Fracture Zone Valley. Site 952 (30°47.45′N, 24°30.57′W; 5431.8 m) is situated in the Cruiser Fracture Zone Valley, more proximal to the source of turbidity currents from the northwest African continental margin than Site 950.

METHODS

Visual Description

Conventional visual core descriptions were carried out aboard the *JOIDES Resolution*, (i.e., barrel sheets; Schmincke, Weaver, Firth, et al., 1995) but, in addition, more detailed descriptions of turbidite units were also made. This was possible because of the distinct color differences between the various units and because a number of the sedimentologists had direct experience of working with cores from this abyssal plain. Logs produced in this way are shown in Figure 2 (back-pocket foldout, this volume). Units that were unidentified or problematic at sea have been re-examined to provide these updated versions.

Correction of Depths

The sub-bottom depths for units within each core have been amended to take account of a number of potential errors (see Lebreiro and Weaver, Chap. 37, this volume). These corrections have generally led to a shortening of the length of recovered sediment in each core and have eliminated all instances of recovered core being longer than the drilled interval. Amendments included:

1. Removal of slumped and disturbed sediment at the top of each core. This material is probably produced by the advance of the main drill bit, and lies on top of the true sediment surface before advanced hydraulic piston (APC) coring commences.
2. Elimination of void spaces. Voids do not exist in the sediment column, and unless material has fallen out of the liner after recovery, the pieces of sediment on each side of a void will be part of an uninterrupted sequence. The voids may be caused by gas expansion or core handling.

These corrections have provided much more accurate methods of assessing the amount of missing sediment, which is vital for determining the frequency of events.

Multisensor Track Data

Nondestructive high-resolution whole-core measurements were obtained aboard ship. The multisensor track (MST) includes gamma-ray attenuation (GRAPE), compressional-wave velocity (PWL), magnetic susceptibility, and multichannel gamma spectrometer sensors (for technical details, see Schmincke, Weaver, Firth, et al., 1995). Magnetic susceptibility was particularly useful for distinguishing between the different types of turbidites since those derived from a volcanic source, such as the Canary Islands, have a much higher signal. Correlation between the three abyssal plain sites was facilitated by comparing the magnetic susceptibility values of particular turbidites since several flows have their own unique signatures.

Calcium Carbonate

Calcium carbonate measurements were made both at sea and ashore using a Coulometrics 5011 Carbon Dioxide Coulometer equipped with a System 140 carbonate carbon analyzer. As with all sampling, an attempt was made to avoid areas of core where bioturbation was visible between adjacent units.

Terminology

Weaver and Kuijpers (1983) began a numbering system for turbidites on the MAP. Laterally extensive turbidites were letter coded a to w from younger to older, and small laterally restricted turbidites were given the letter of the turbidite above with a numbered suffix. These codes are shown in the correlation diagram (Fig. 2, back-pocket foldout, this volume) but the system has not been extended to the deeper turbidites.

SEDIMENT TYPES

In the MAP, the sedimentary infilling consists primarily of turbidite units separated by much thinner pelagic layers with occasional debris flows. In the MAP it is rare to find two turbidites adjacent to each other. They are almost always separated by a pelagic layer representing a few tens of thousands of years (Weaver et al., 1992).

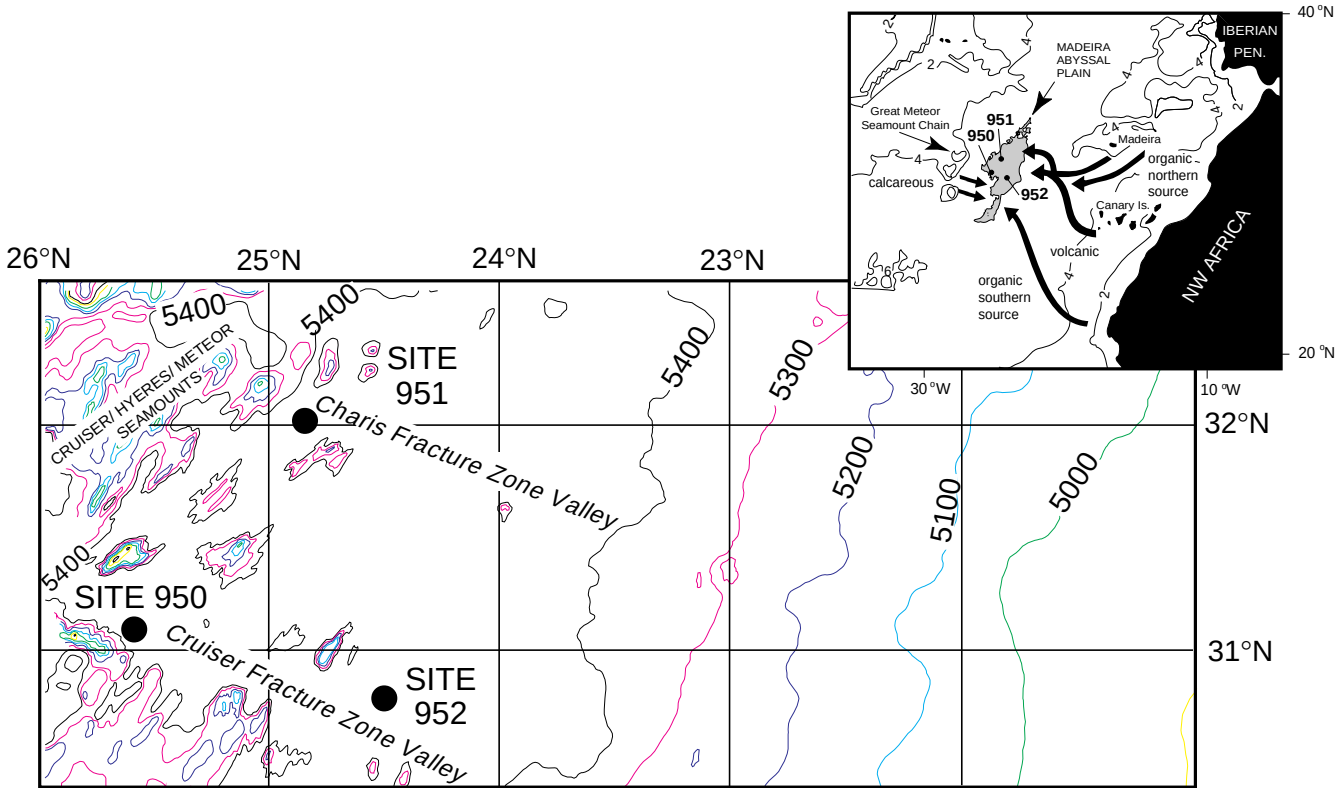

Figure 1. **Top:** Geographical context of the Madeira Abyssal Plain, showing the sources of turbidite flows. **Bottom:** Locations of the three sites drilled on the Madeira Abyssal Plain with topographic elevations. The 5400-m contour outlines the edge of the plain.

Pelagic Sedimentation

Pelagic layers vary from a few centimeters to 0.5 m in thickness. Their composition varies from almost pure carbonate ooze (up to 93% $CaCO_3$ in some lower Pleistocene layers), to pure pelagic clay with 0% $CaCO_3$ (Fig. 3). Pelagic clay was deposited continuously from the late Eocene to the late Miocene, around 8 Ma, at which time a few layers show carbonate values of up to 30%, although these are interspersed with pure clay layers. Through the lower Pliocene interval, $CaCO_3$ values are around 20%, but there is a dramatic change at 115 mbsf (Site 950), ~3.5 Ma, when strong oscillations begin. At first these layers show changes between 20% to 65% $CaCO_3$, but variability rapidly increases from 5% to 85% with a number of layers having intermediate values. There appears to be a preservation peak between 75 and 15 mbsf (~2.0 to 0.5 Ma) in which several ooze layers were deposited with over 80% $CaCO_3$, although these were interlayered with marls and clays. Since 0.5 Ma, the highest carbonate values have remained less than 70% (Fig. 3). This picture of $CaCO_3$ oscillation reflects the changes in ocean circulation through the Neogene. The calcium carbonate compensation depth (CCD) began to deepen slightly during the late Miocene and again in the early Miocene (≈5 Ma), and around 3.5 Ma the CCD depth began to oscillate dramatically in phase with the Pliocene/Pleistocene glaciations. Weaver and Kuijpers (1983) showed that the pelagic clay layers in the MAP were deposited during glacials, whereas the marls and oozes were deposited during interglacials. The dramatic and sharp changes in $CaCO_3$ preservation between glacials and interglacials may be caused by reversals in the circulation of the Atlantic Ocean (Broecker et al., 1990). During interglacials relatively noncorrosive bottom waters generated in the Greenland-Norwegian Sea flow southward, displacing Antarctic Bottom Water (AABW) and allowing carbonate to accumulate in the deep basins. The flow is compensated by a northward movement of surface water that carries heat to high latitudes. During glacials the surface water moves southward and deep corrosive AABW spreads north, thus raising the CCD. Broecker et al. (1990) suggest these reversals in flow could be sudden, which appears to be supported by the sharp changes from clay to ooze/marl seen in the cores. Our data suggest that prior to the Pliocene/Pleistocene glaciations, the CCD was more stable, although its level changed a few times through the late Miocene and early Pliocene. The preservation peak in the lower Pleistocene has been noted earlier by Jansen et al. (1986). A more thorough analysis of $CaCO_3$ fluctuations is underway (Weaver et al., unpubl. data).

Turbidites

The three turbidite groups mentioned in the "Introduction" section (this chapter) were found at all three sites. They show some variation through time, and in the deeper parts of the sequence, other turbidite groups are also present. We will therefore discuss the sedimentary characteristics of each turbidite group through time.

The complete sedimentary sequence for each site is shown in Figure 2 (back-pocket foldout, this volume), together with some of the many correlations between individual flows. A summary of the main lithologic changes is presented in Figure 4.

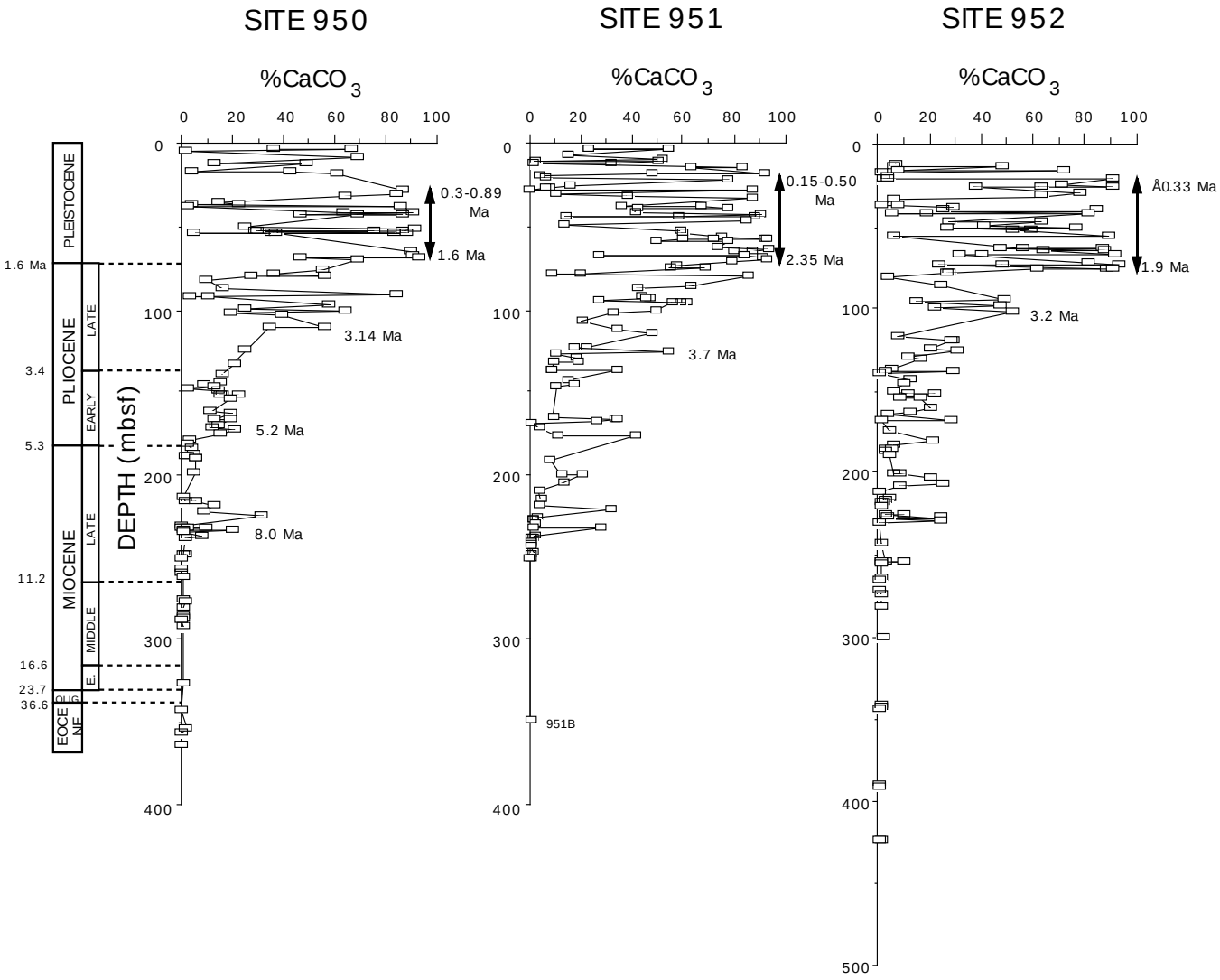

Figure 3. Calcium carbonate oscillations from the pelagic interbeds at Sites 950, 951, and 952. Note only a small number of the pelagic layers were sampled. In the Pliocene–Pleistocene sediments, there are many more fluctuations in $CaCO_3$ than shown here.

Organic Turbidites

These turbidites are characterized by high organic carbon content (>0.3%; De Lange et al., 1987) giving green colors, very low magnetic susceptibility (<20 cgs) and variable carbonate content. They range in composition from clays to nannofossil clays and clayey nannofossil mixed sediments (Schmincke, Weaver, Firth, et al., 1995) with the principal components being clay minerals, nannofossils, and lesser amounts of quartz, dolomite, feldspar, pyrite, foraminiferal test fragments, and biosiliceous material. Minor amounts of silt-sized material are found throughout the muds, suggesting they are ungraded, falling into the E3 turbidite mud division of Piper (1978). Silt-sized material is more common toward the bases of units with laminated or graded layers. The bases frequently contain complete benthic and planktonic foraminifers. These organic turbidites show the classic oxidation fronts of Wilson et al. (1985), with pale green tops and darker green bases, and frequently have a series of thin color bands marking intervals of metal enrichment in the oxidation front itself. Individual turbidites range from a few centimeters to 3–4 m in thickness.

There is a relationship between color and carbonate content (Fig. 5). Three shades of green are observed: dark-green turbidites, present mainly below 220 mbsf in each site, always correspond to <40% $CaCO_3$; intermediate green turbidites appear through the whole column, but contain 40%–60% $CaCO_3$ above 220 mbsf and <40% below 220 mbsf; and finally pale-green turbidites that contain 40%–70% $CaCO_3$.

High organic content suggests that these turbidites derived from upwelling areas on the northwest African Margin (see Fig. 1). They are unlikely to have derived from possible upwelling around the Canaries or Madeira because they all have very low magnetic susceptibilities in contrast to the volcanic-rich sediments on the island flanks. Biogenic siliceous debris, mainly diatoms and sponge spicules, is present in rare to common abundance at all three sites through nannofossil Subzone CN5a and Zone 4 (12.2–16 Ma).

It has been possible to correlate many of the individual organic-rich turbidites between the three sites as shown in Figure 2 (back-pocket foldout, this volume). Through the upper Miocene to Holocene sediments, all the major units can be correlated, but below this there is a distinct difference between Site 950 and Sites 951 and 952.

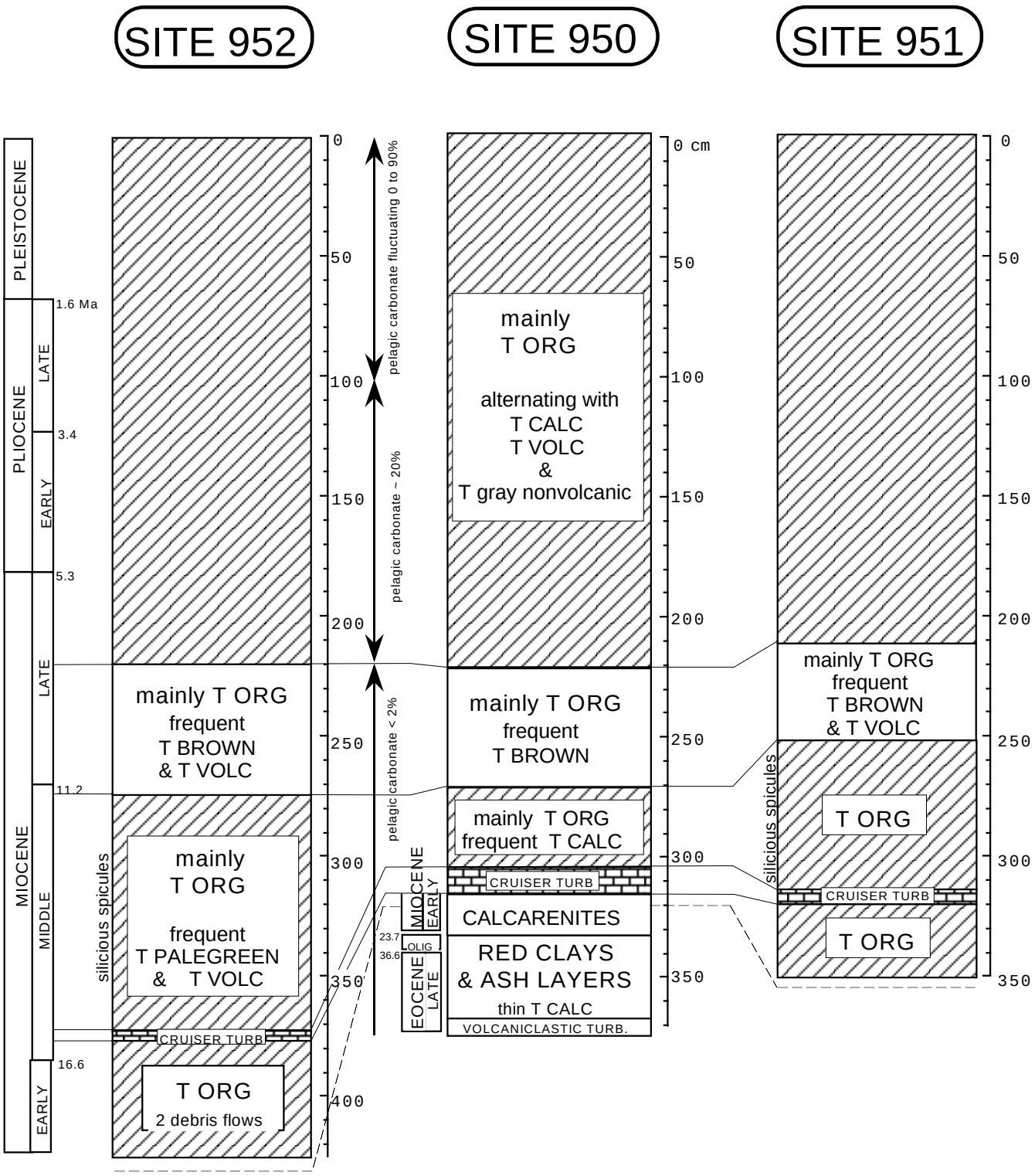

Figure 4. Summary of main lithologic changes at Sites 950, 951, and 952. Prior to the Cruiser Turbidite deposit, different sediments filled independent fracture zone valleys. From the early Miocene sequence, above the Cruiser Turbidite, the plain was overflowed as a whole; therefore, the lithologic units are similar between sites, except for the local contributions marked in the drawing. Based on the general correlation chart in Figure 2 (back-pocket foldout, this volume). T = turbidite, ORG = organic-rich turbidites, CALC = calcium carbonate-rich turbidites, and VOLC = volcanic-rich turbidites.

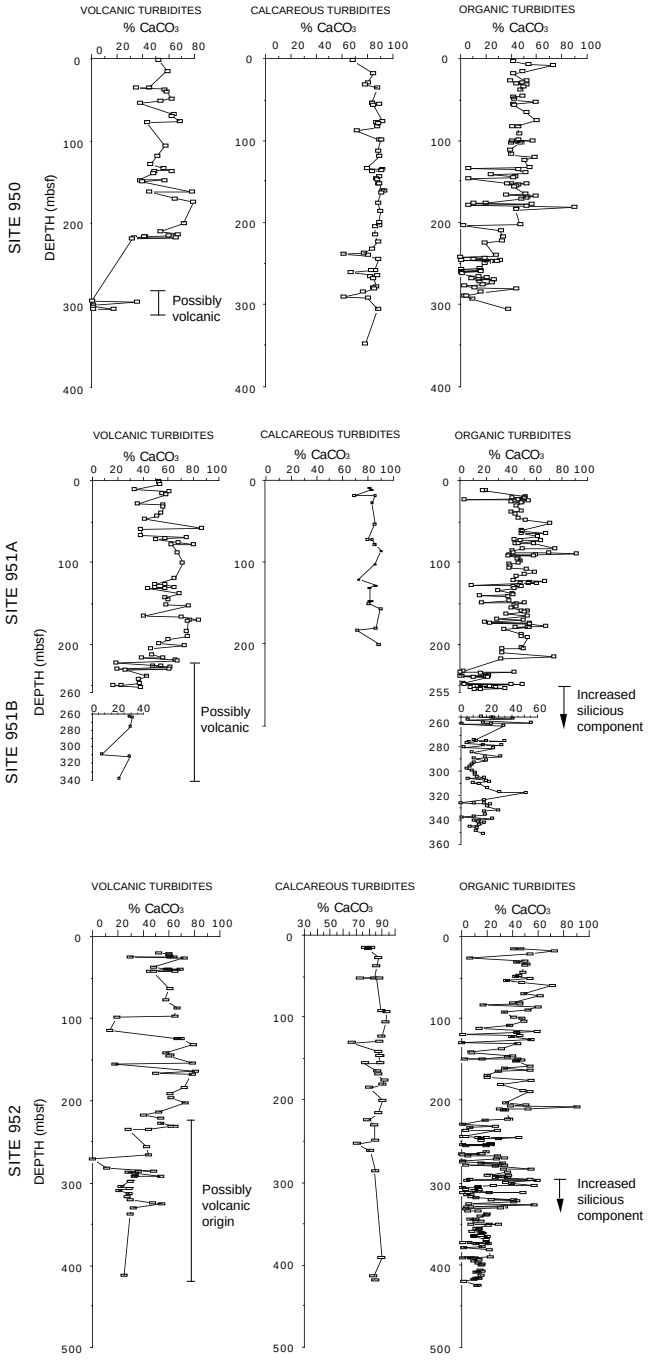

Figure 5. Calcium carbonate values for a selection of organic, volcanic, and calcareous turbidites at Sites 950, 951, and 952.

The latter two sites show much more frequent deposition of green turbidites (generally less than 1 m thick).

Pale-green turbidites were emplaced very frequently during the middle Miocene (16–12 Ma), ranging in thickness between 0.08–0.60 m, and less frequently during the Pliocene (5.3–2 Ma), but with thicknesses up to 3.7 m. In both periods, the pale-green turbidites are preferentially deposited at Site 952, according to its proximity to the source area.

In all three sites there is a distinct change in $CaCO_3$ content of the organic turbidites at ~6.5 Ma (~210 mbsf at each site). Below these levels many organic turbidites have $CaCO_3$ values below 20%, whereas above these levels most turbidites have $CaCO_3$ values of 30%–60% (Fig. 5). This change in carbonate content slightly postdates the increase in pelagic carbonate preservation seen at each site, and may indicate a large regional deepening of the CCD. It is possible that some of the source areas of the organic turbidites were below the CCD before this event and thus were giving rise to low calcium carbonate turbidites.

Volcanic Turbidites

These turbidites are characterized by high magnetic susceptibility (>100 cgs) due to the presence of volcanic minerals. They are gray in color, contain little or no organic carbon, and show a wide range of $CaCO_3$ contents. The color and carbonate content seem to be related, with the darker gray units having lower calcium carbonate contents. The silt fractions of the volcanic turbidites contain anhedral feldspar, pyroxenes, and volcanically derived accessory minerals, as well as felsic volcanic glass shards in some units. Individual turbidites range from a few centimeters to several meters thick, and all the larger flows have been correlated between the three sites (Fig. 2, back-pocket foldout, this volume).

Volcanic turbidites are very rare in the deeper parts of each site through the middle and lower part of the upper Miocene sediments. In these intervals any gray turbidites are difficult to classify as volcanic because of their low magnetic susceptibility. They are, however, very thin, averaging only a few centimeters to a few tens of centimeters in thickness. Beginning ~7 Ma (~220 mbsf at each site), the volcanic turbidites suddenly become much thicker and show distinctive high magnetic susceptibility values (Fig. 2, back-pocket foldout, this volume). From this level to the hole tops, the volcanic turbidites can be easily correlated among the three sites. The volcanic turbidites younger than 7 Ma have $CaCO_3$ values ranging between 30%–80%, but older than this, the few thin questionable volcanic units vary from 0%–60% $CaCO_3$.

The upper Eocene and Oligocene intervals at Site 950 comprise red clays with some thin brown turbidites and numerous volcanic ash layers. This whole interval has a very high magnetic susceptibility. The volcanic components here are all believed to derive from the chain of seamounts to the west of the MAP (Cruiser/Hyeres/Great Meteor Chain), which we know were active volcanoes during the early Neogene (Schmincke, Weaver, Firth, et al., 1995).

Gray Nonvolcanic Turbidites

This group of turbidites shows strong similarities to the volcanic group in terms of color, $CaCO_3$ and organic carbon content. However, they show very low magnetic susceptibilities, which suggests that they do not have a volcanic component. Element composition analysis (Jarvis et al., Chap. 31, this volume) shows higher K/Al ratio (0.35:0.25) and much lower Ti/Al ratio (0.06:0.08–0.20) as the differences between nonvolcanic and organic and volcanic turbidites, respectively. The nonvolcanic turbidites are among the thickest turbidites recovered, exceeding 11 m at Site 952 (200.03–188.86 mbsf).

They occur in four principal groups. The first group, 12.5–11.5 Ma, comprises a few turbidites between 260 and 253 mbsf, the second group was deposited during the interval 7.4–5.6 Ma and includes turbidites between 232 and 185 mbsf, the third group dates from 4.2–3.8 Ma and comprises turbidites between 152 and 144 mbsf, and finally, group four took place between 1.6 and 1.4 Ma, turbidites 65–51 mbsf. The oldest group is only represented at Site 951, whereas the other groups are large flows that can be correlated between the three sites (Fig. 2, back-pocket foldout, this volume).

We do not know the source of these turbidites, but their ages slightly postdate the origin of the volcanic Canary islands of Gran Canaria and Lanzarote, Tenerife, and La Palma and Hierro (Schmincke, 1994). It is possible that the early submarine develop-

ment of a volcanic island is associated with doming of the sediment pile leading to mass wasting of sediments rather than volcanic material.

Volcaniclastic Turbidites

These turbidites are represented by two distinctive flows at the base of Hole 950A (Fig 2, back-pocket foldout, this volume). They consist of volcaniclastic silt and fine-grained sandstone capped by greenish gray clay of probable turbidite origin. The silt/sand parts are planar and trough cross-laminated with the lower turbidite grading down into massive sand. They consist mainly of volcanic basaltic rock fragments and glass shards with only a small admixture of calcareous reworked microfossils. Their nature and composition suggest they were locally derived from erosion of the Cruiser/Hyeres/Great Meteor Seamount chain to the west.

Calcareous Turbidites

These turbidites are white and show $CaCO_3$ contents of more than 80% and have negligible organic carbon content and low magnetic susceptibility. They are composed dominantly by nannofossils, and where they have coarser bases they are composed of foraminiferal tests. They vary from a few centimeters to ~3.6 m thick and are volumetrically less important than either the organic or volcanic turbidites. These turbidites derived from the seamounts to the west of the MAP (Weaver et al., 1992) and are funneled into the plain through the fracture zone valleys. As a consequence, there are more calcareous turbidites in the proximal Site 950, and these have more frequent and thicker sandy bases than the calcareous turbidites at Site 952, which lies distally along the same fracture zone valley. The thicker calcareous turbidites can be correlated between the three sites (Fig. 2, back-pocket foldout, this volume).

Recovery is poor between 308 and 332.5 mbsf at Site 950 (Cores 157-950A-34X through 36X), but this interval does contain two calcarenite units and a thick calcareous turbidite. The downhole logs show this interval to consist of three separate graded beds lying between 308–318.5, 322–324.5, and 326–332.5 mbsf. The upper one of these flows is widespread and distinctive, so we have named it the Cruiser Turbidite, after the Cruiser Seamount. The basal part of the Cruiser Turbidite consists of sand-sized carbonate grains mixed with volcanic debris and granule- to pebble-sized clasts of greenish clay up to 3 cm in diameter. The neritic calcareous grains are strongly reminiscent of calcareous beach sand, and the volcanic material is very fresh, indicating that this deposit was eroded from a beach soon after a volcanic eruption. The incorporation of clay clasts suggests these were ripped up from the seabed at depths below the CCD. The mud part of the Cruiser Turbidite at Site 950 grades from a brown carbonate-poor mud to a white carbonate-rich mud, again implying a mixture of sediment from well above and well below the CCD.

The Cruiser Turbidite has been correlated between all three sites. At Site 951 it is 3.6 m thick with 0.51 m of wackestone at its base. It grades from white in the lower part to green at the top and from 71% $CaCO_3$ in the lower calcareous mudstone to 31% $CaCO_3$ in the green upper part. At Site 952 it is 3.92 m thick with 0.88 m of graded sand and silt at its base. It again grades from a white calcareous mudstone with $CaCO_3$ content of 81% to a green mud at the top with a $CaCO_3$ content of 27%. It appears that this unit caused considerable erosion on the plain, eroding pelagic clay on its approach to Site 950 and then green abyssal plain turbidites as it progressed toward the locations of Sites 951 and 952. These clays and green muds appear to be finer grained than the original pelagic sediment and concentrated at the top of the unit during its deposition.

Brown Turbidites

These turbidites are brown, have moderately high magnetic susceptibility, $CaCO_3$ values ranging from 5%–70%, and low organic carbon content. Two shades of brown are observed: pale brown and greenish brown, both with $CaCO_3$ content of 20%–50%. These turbidites occur only in the interval between 215–281 mbsf at Site 950 (~6.5–13 Ma). At Sites 951 and 952 they are not so well represented. The moderately high magnetic susceptibility of these turbidites may be indicative of higher pelagic clay content since the pelagic clay layers between turbidites have high magnetic susceptibility. It would also account for their brown color. Because they are more common at Site 950 to the west of the plain, we assume that they derive from the seamounts to the west. They presumably have a deeper water origin than the calcareous turbidites from this source. We do not know why they should occur over a limited time interval, although the deepening of the CCD progressively after 8 Ma may have altered sedimentation in their source from clay to ooze.

Debris Flows

Debris flows were identified only in the lower Miocene sediments, and exclusively at Site 952. The unit between 386.64–386.81 mbsf (Core 157-952A-43X) consists of indurated dark-gray sand-supported clasts, which fall into two classes: subrounded, millimeter-sized bluish green mud clasts and angular, planar, up to 7 cm long, dark-gray clayey silt clasts with siliceous microfossils, foraminifers, and nannofossils. The clasts are horizontally oriented. The unit grades up into a green turbidite and has a total thickness of 7.11 m. A second debris flow with a thickness of 1.88 m occurs in Core 157-952A-43X.

HISTORY OF BASIN INFILL

The history of basin infill is summarized in Figure 6, where the contribution from each of the main sources: northwest African Margin, Canary Islands, Cruiser/Hyeres/Great Meteor Seamount Chain, is given for each site. Site 950 extends furthest back in time reaching the upper Eocene (Howe and Sblendorio-Levy, Chap. 29, this volume). The oldest sediments cored include two coarse-grained volcaniclastic turbidites that appear to have derived from the now-extinct volcanoes of the Cruiser/Hyeres/Great Meteor Seamount Chain to the west. The vesicular nature of the altered vitric tuffs, together with oxidized scoria fragments, indicate that some of the material was derived from subaerial volcanism. The rest of the upper Eocene and Oligocene is represented by red clay. Numerous zeolitic ash-fall layers within this sequence suggest the proximity of active volcanoes, almost certainly the Great Meteor/Cruiser/Hyeres Chain, and the occurrence of thin brown turbidites evokes instability of the volcano flanks. These turbidites contain some volcaniclastic silt and an abundance of smectite clays, indicating alteration of volcanic glass. Thus, the seamount chain to the west of the MAP was volcanically active until at least the end of the Oligocene. There is no evidence of locally derived volcanic material after this time, but there is a 8.3-m.y. hiatus (see Howe and Sblendorio-Levy, Chap. 29, this volume) during which a large part of the lower Miocene sequence could have been removed.

Above the lower Miocene hiatus at Site 950 are the three calcarenites that were again derived from the seamounts to the west. It is likely that these coarse flows caused the erosion of the lower Miocene sediments. They contain shallow water or beach material, suggesting that the seamounts were still subaerial. The lowest of these calcarenites has an age of 17 Ma (Howe and Sblendorio-Levy, Chap. 29, this volume), which is slightly older than the basal sediments at Sites 951 and 952. The thick upper flow—the Cruiser Turbidite—has

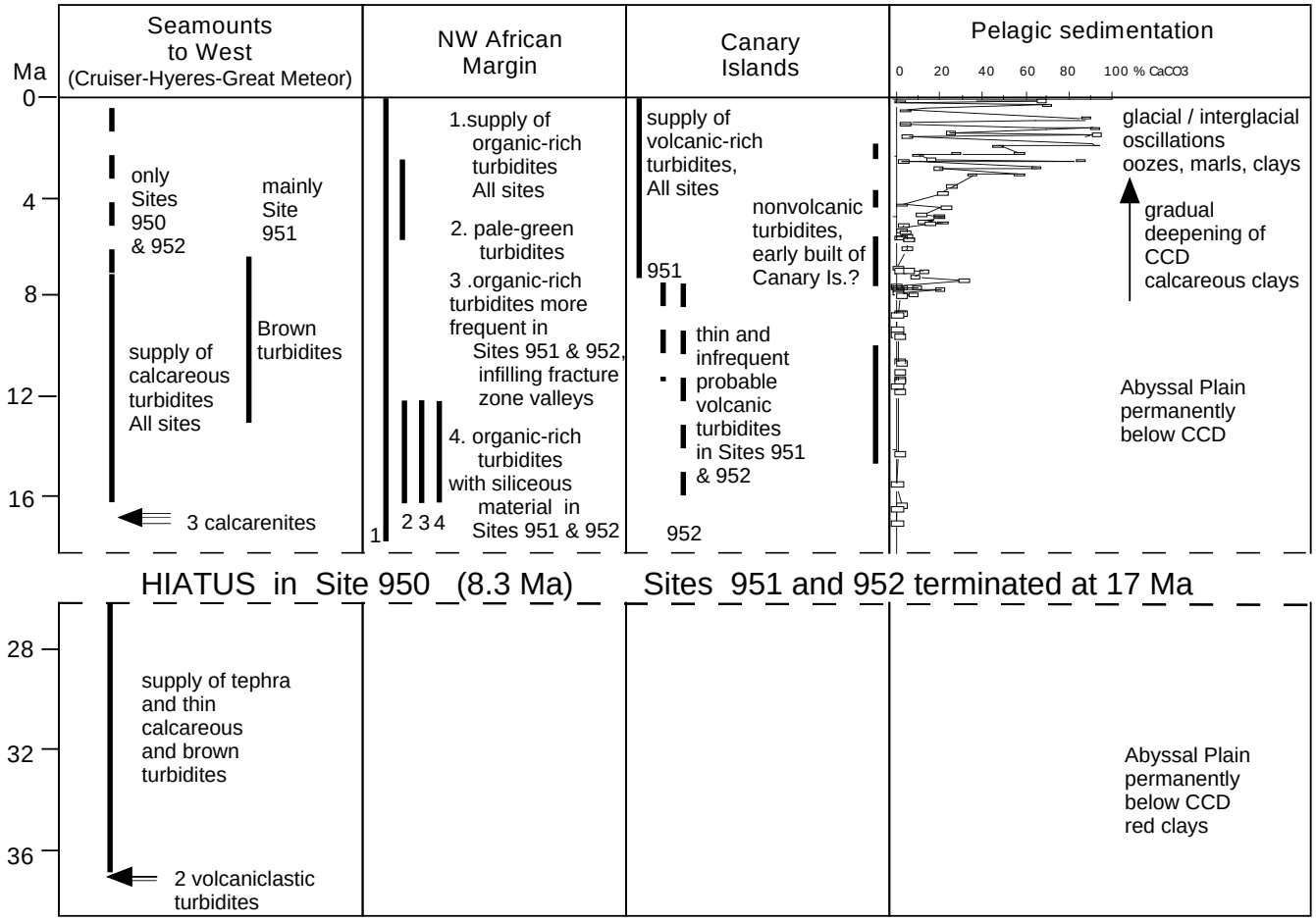

Figure 6. History of basin development showing the contribution of each of the main sediment sources through time.

been correlated across the basin. At Sites 951 and 952 the sequence below the Cruiser Turbidite consists of numerous green turbidites, mostly less than a meter thick, and emplaced at a high frequency. These turbidites are not found at Site 950, and even above the Cruiser Turbidite, the frequency of green turbidite emplacement is greater at Sites 951 and 952. These latter two sites are situated over the center of a fracture zone valley, and Site 950 is located more to the valley side. Seismic data (Rothwell et al., this volume) shows that the turbidite sequence is much thicker in the fracture zones, and it appears that this is due to the early infilling of the fracture zone valleys during the late early and middle Miocene. The occurrence of debris flows in the lower Miocene sediments of Site 952 suggests that this site lay at the base of the continental slope during the early Miocene, rather than some distance across the abyssal plain. After ~16 Ma, turbidites began to spread across the whole area and the plain began to form. The fact that these turbidites, which now cover a much larger area, are of equal or greater thickness to those involved in the fracture zone filling, suggests a large increase in the volume of each individual flow.

The deeper organic turbidites of Sites 951 and 952 (older than ~12 Ma) contain significant amounts of biosiliceous material, in contrast to the organic turbidites above, which supports either a change in the dominant plankton types living along the northwest African Margin from siliceous to calcareous, or a change in the potential preservation of siliceous material.

From the base of the upper Miocene sediments to the Holocene, it is possible to correlate many of the turbidites among the three sites. At ~7 Ma volcanic turbidites were suddenly deposited in the sequence. A few thin, gray turbidites older than this were not conclusively identified as volcanic. We do not know why the deposition of volcanic turbidites should have begun at 7 Ma. The most likely source of all such flows is the Canary Islands (Weaver et al., 1995; Masson, 1996), but these have a history extending back to 20 Ma (Schmincke, 1994). The islands, in fact, have an age progression from east to west with Fuerteventura having an age of 20 Ma and Hierro in the west being less than 2 Ma. It is possible that turbidites shed from the older eastern islands of Lanzarote, Fuerteventura, and Gran Canaria were trapped in a local basin that had filled by 7 Ma. Alternatively, the birth of Tenerife at this time (5–7 Ma, Ancochea et al., 1990) may have breached the western margin of this local basin, thus allowing flows to travel further west to the MAP. The latter hypothesis is supported by the fact that the first flows are both thick and frequent, accounting for a sudden event rather than a gradual basin filling, which would have allowed the larger flows to overflow with increasing force.

The amount of $CaCO_3$ in the pelagic layers began to rise at ~8 Ma, indicating a regional deepening of the CCD at this time. Other steplike increases in $CaCO_3$ preservation occur at ~5 and 3.5 Ma. From 3.5 Ma to the present day there have been very large oscillations in the preservation of $CaCO_3$ linked to bottom-water changes associated with Pliocene–Pleistocene glaciations. The first increase in preservation at 8 Ma is associated with an increase in the average $CaCO_3$ content of the organic and volcanic turbidites at this time, which leads us

to consider that at least part of the source areas of each was previously affected by dissolution. The brown turbidites with relatively low $CaCO_3$ contents also disappear at ~8 Ma.

ACKNOWLEDGMENTS

We thank Stephen Pink for carrying out many of the calcium carbonate analyses. This work was supported by the European Commission on Marine Science and Technology (MAST II) through the STEAM program grant MAS2-CT94-0083 and NERC grant No. GST/02/990.

REFERENCES

Ancochea, E., Fúster, J.M., Ibarrola, E., Cendrero, A., Coello, J., Hernán, F., Cantagrel, J.M., and Jamond, C., 1990. Volcanic evolution of the island of Tenerife (Canary Islands) in the light of new K-Ar data. *J. Volcanol. Geotherm. Res.,* 44:231–249.

Broecker, W.S., Bond, G., Klas, M., Bonani, G., and Wolfi, W., 1990. A salt oscillator in the glacial Atlantic? 1. The concept. *Paleoceanography,* 5:469–477.

De Lange, G.J., Jarvis, I., and Kuijpers, A., 1987. Geochemical characteristics and provenance of late Quaternary sediments from the Madeira Abyssal Plain, North Atlantic. *In* Weaver, P.P.E., and Thomson, J. (Eds.), *Geology and Geochemistry of Abyssal Plains.* Geol. Soc. Spec. Publ. London, 31:147–165.

Duin, E.J.T., and Kuijpers, A., 1983. *Geological Studies on Abyssal Plains in the North Atlantic:* Contrib. Seabed Working Group Progr. Rept. 1982, Internal Rept.: Haarlem (Rijks Geol. Dienst).

Jansen, J.H.F., Kuijpers, A., and Troelstra, S.R., 1986. A mid-Brunhes climatic event: long-term changes in global atmospheric and ocean circulation. *Science,* 232:619–622.

Jarvis, I., and Higgs, N., 1987. Trace-element mobility during early diagenesis in distal turbidites: late Quaternary of the Madeira Abyssal Plain, N Atlantic. *In* Weaver, P.P.E., and Thomson J. (Eds.), *Geology and Geochemistry of Abyssal Plains.* Geol. Soc. Spec. Publ. London, 31:179–214.

Masson, D.G., 1996. Catastrophic collapse of the volcanic island of Hierro 15 ka ago and the history of landslides in the Canary Islands. *Geology,* 24:231–234.

McCave, I.N., and Jones, K.P.N., 1988. Deposition of ungraded muds from high-density non-turbulent turbidity currents. *Nature,* 333:250–252.

Piper, D.J.W., 1978. Turbidite muds and silts on deepsea fans and abyssal plains. *In* Stanley, D.J., and Kelling, G. (Eds.), *Sedimentation in Submarine Canyons, Fans and Trenches:* Stroudsburg, PA (Dowden, Hutchinson and Ross), 163–175.

Schmincke, H.-U., 1994. *Geological Field Guide: Gran Canaria* (7th ed.): Kiel, Germany (Pluto Press).

Schmincke, H.-U., Weaver, P.P.E., Firth, J.V., et al., 1995. *Proc. ODP, Init. Repts.,* 157: College Station, TX (Ocean Drilling Program).

Searle, R.C., 1987. Regional setting and geophysical characterization of the Great Meteor East area in the Madeira Abyssal Plain. *In* Weaver, P.P.E., and Thomson, J. (Eds.), *Geology and Geochemistry of Abyssal Plains.* Spec. Publ. Geol. Soc. London, 31:49–70.

Thomson, J., Colley, S., Higgs, N.C., Hydes, D.J., Wilson T.R.S., and Sorensen, J., 1987. Geochemical oxidation fronts in NE Atlantic distal turbidites and their effects in the sedimentary record. *In* Weaver, P.P.E., and Thomson, J. (Eds.), *Geology and Geochemistry of Abyssal Plains.* Geol. Soc. Spec. Publ. London, 31:167–177.

Verhoef, J., and Collette, B.J., 1983. A tear fault system beneath the Atlantis-Meteor Seamount Group. *Ann. Geophys.,* 1:199–206.

Weaver, P.P.E., and Kuijpers, A., 1983. Climatic control of turbidite deposition on the Madeira Abyssal Plain. *Nature,* 306:360–363.

Weaver, P.P.E., Masson, D.G., Gunn, D.E., Kidd, R.B., Rothwell, R.G., and Maddison, D.A., 1995. Sediment mass-wasting in the Canary Basin. *In* Pickering, K.T., Hiscott, R.N., Kenyon, N.H., Ricci Luchi, F., and Smith, R.D.A. (Eds.), *Atlas of Deep Water Environments: Architectural Style in Turbidite Systems:* London (Chapman and Hall), 287–296.

Weaver, P.P.E., and Rothwell, R.G., 1987. Sedimentation on the Madeira Abyssal Plain over the last 300,000 years. *In* Weaver, P.P.E., and Thomson, J. (Eds.), *Geology and Geochemistry of Abyssal Plains.* Geol. Soc. Spec. Publ. London, 31:71–86.

Weaver, P.P.E., Rothwell, R.G., Ebbing, J., Gunn, D., and Hunter, P.M., 1992. Correlation, frequency of emplacement and source directions of megaturbidites on the Madeira Abyssal Plain. *Mar. Geol.,* 109:1–20.

Weaver, P.P.E., Thomson, J., and Jarvis, I. 1989. The geology and geochemistry of Madeira Abyssal Plain sediments: a review. *In* Freeman, T.J. (Ed.), *Advances in Underwater Technology, Ocean Science and Offshore Engineering* (Vol. 18): London (Graham and Trotman), 51–78.

Wilson, T.R.S., Thomson, J., Colley, S., Hydes, D.J., Higgs, N.C., and Sorensen, J., 1985. Early organic diagenesis: the significance of progressive subsurface oxidation fronts in pelagic sediments. *Geochim. Cosmochim. Acta.,* 49:811–822.

Date of initial receipt: 3 July 1996
Date of acceptance: 8 March 1997
Ms 157SR-128